

Brickwork under eccentric compression: Experimental results and macroscopic models

Antonio Brencich^{a,1}, Gianmarco de Felice^{b,*}

^a University of Genova, Department of Civil, Architectural and Environmental Engineering, via Montallegro 1, 16145 Genova, Italy

^b University Roma Tre, Department of Structures, via Corrado Segre 6, 00146 Rome, Italy

ARTICLE INFO

Article history:

Received 6 August 2007

Received in revised form 2 September 2008

Accepted 4 September 2008

Available online 31 October 2008

Keywords:

Masonry

Solid clay brickwork

Eccentric loading

Arches

Arch bridges

Constitutive models

Assessment

ABSTRACT

The compressive strength of masonry is a relevant mechanical parameter playing a central role in the assessment of masonry structures. In spite of a large number of experimental data and theoretical approaches, the failure of brickwork pillars and arches, its dependence on the properties of the constituents and on the loading conditions is not yet clear. In this paper, the compressive response of solid clay brick masonry is analyzed on the basis of a series of experimental tests performed on brickwork prisms made with different constituents, either old and new clay bricks arranged with cement and lime mortar, subjected to both concentric and eccentric loading with different load eccentricities. The tests have been displacement controlled in order to reproduce, in terms of both load–displacement and moment–curvature diagrams, the whole response curve, including the post-peak branch. According to the plane section hypothesis, one-dimensional constitutive models of brickwork, suitable for engineering application, are formulated to represent the non-linear behaviour of masonry. The comparison between theoretical predictions and experimental data, also derived from literature, represented in the axial force–bending moment failure domain, point at the adequacy of the models in estimating the load bearing capacity under eccentric loading, provided that the inelastic response is properly taken into account.

© 2008 Elsevier Ltd. All rights reserved.

1. Introduction

The load carrying capacity of masonry structures under eccentric loading is a primary issue for the assessment of several structural elements, such as walls, vaults, arches and pillars. Even though these structures are quite different, they may exhibit a stress concentration resulting from the eccentricity of the load, which may lead to the crushing failure of the material. With the classical assumption of no-tensile-resistance (NTR) with a perfectly brittle (PB) compressive behaviour, as reported by different authors [1–6] an increase, up to twice the value for concentric loading, of the material compressive strength needs to be assumed for eccentric loading to fit the experimental results. The UIC code 778-3R [7] allows an increase of the material strength for eccentric loading up to 60% of the concentric value.

According to its mechanical meaning, the compressive strength of masonry has to be considered as a constitutive parameter that is independent on the load condition; for this reason, the increase of the material strength for eccentric loading, points out the inadequacy of a perfectly brittle model to reproduce the compressive behaviour of masonry under non-uniform stress states. As shown

by some authors [8–10] the fitting of eccentric tests can be obtained by taking into account the inelastic response of masonry, rather than with an unexplained increase of the material compressive strength.

Since inhomogeneous stress and strain fields are expected under compression, a detailed and comprehensive model should consider masonry as a composite medium with different constituents (mortar, bricks and brick/mortar interfaces) taking into account the actual geometry of brickwork (size of the bricks, thickness of the joints and masonry bond) and the effective loading condition. However, at the scale of a structural element, i.e. of wall or an arch, this approach may result computationally unfeasible and masonry may be represented as a homogeneous material described in terms of mean strain and mean stress fields. While the overall stiffness may be defined by means of appropriate homogenization techniques, the overall strength remains strongly dependent on stress concentrations at the mesoscale. The first proposed models [11–14 among the others] refer to brickwork as compressed unbonded layered medium: strain compatibility conditions at the brick/mortar interface result in horizontal transversal tractions in the brick, responsible of the collapse of the brick layer. Despite of the clear interpretation of compressive failure provided by these models, the assumption of layered material, that neglect both, mortar head joints and boundary conditions, limits the reliability of the results [10,15]. Improvements of these models for compressed brickwork [16,17] are based on an application of the static theorem of limit

* Corresponding author. Tel.: +39 06 55176268; fax: +39 06 55176265.

E-mail addresses: brencich@dicat.unige.it (A. Brencich), defelice@uniroma3.it (G. de Felice).

¹ Tel.: +39 010 3532512; fax: +39 010 3532534.

analysis to a prescribed local stress field in the representative volume element. Nevertheless, the approach cannot be easily generalised to correctly reproduce boundary effects and/or stress field under eccentric loading and, therefore, these models often fail in providing a clear representation of the collapse mechanism together with an accurate prediction of brickwork strength under eccentric compression.

In this paper, aiming at investigating the load carrying capacity of brickwork under eccentric loading, a series of experimental tests have been performed with different load eccentricity, ranging from 0 (concentric tests) to 80 mm (1/3rd of the brick length); the tests have undergone with displacement control for recording also the post-peak descending branch of the load–displacement curve (Section 2). In order to find out the dependency of the load–displacement behaviour on the material (brick and mortar) properties, the experimental tests have been repeated using three different kinds of masonry prisms made either with historical bricks manufactured with hydraulic lime mortar, and modern bricks with two different kinds of cement–lime mortar. The results of the tests (Section 3) have been used to formulate phenomenological non-linear constitutive models, suitable for engineering assessment of masonry arches and pillars under combined axial load and bending. The models (Section 4) have been developed under the following assumptions: (i) masonry is represented by an equivalent homogeneous material; (ii) the Navier hypothesis of plane cross-sections is valid; (iii) a uniaxial constitutive model is considered; (iv) masonry has a vanishing tensile strength (no-tensile-resistance, NTR).

The approaches differ in the uniaxial constitutive law assumed in compression which are: (a) elastic–perfectly brittle (NTR-PB), [18]; (b) elastic–perfectly plastic (NTR-PP); (c) elastic–perfectly plastic with limited ductility (NTR-EP), [9]; (d) Kent and Park model (K&P), [19]. Although these models give only a simplified phenomenological description of masonry under compression, they provide an easy estimate of the limit strength domain in the axial force–bending moment plane that can be used in the assessment of structural elements such as arches, bridges [20], pillars and walls. The accuracy of the different approaches is then verified through the comparison with experimental results (Sections 5–7).

2. Testing procedures

2.1. Experimental program, specimens and materials

Two types of specimens made with three types of brickwork have been tested in the context of the present experimental program:

Table 1
Composition and relevant properties of mortars

Property	Mortar 1	Mortar 2	Mortar 3
Density (kN/m ³)	18.5	18.0	16.0
Max aggregate diameter (mm)	3	3	0.6
Water content (% in weight)	18	19	22
Binder/aggregate ratio	See note	See note	1/4
Sand type	Graded	Siliceous	Graded siliceous pit
Classification	M5 – prEN 998-2	M5 – prEN 998-2	NHL5 – prEN459-1

Note: mortars 1 and 2 are industrial pre-mixed products for which the manufacturer (Fassa Bortolo) refused to provide the exact binder-to-aggregate ratio. The commercial names for mortar 1 and mortar 2 are MM30 and MB49, respectively.

- specimen type 1: 110 × 250 × 270 mm prism of four bricks and five mortar joints (10 mm thick), made with brickwork 1 and 2 (Fig. 1a) and
- specimen type 2: 140 × 280 × 300 mm prism of five bricks and six mortar joints (8 mm thick), made with brickwork 3 (Fig. 1b).

The brickwork characteristics are reported hereafter:

- brickwork 1: 55 × 110 × 240 mm modern bricks used for the restoration of historical buildings + mortar 1 (cement–lime);
- brickwork 2: same bricks as brickwork 1 + mortar 2 (“white” cement–lime) and
- brickwork 3: 140 × 280 × 55 mm bricks (produced in the clink of Monterotondo, close to Rome, at the beginning of 20th century) + mortar 3 (hydraulic lime mortar).

Table 1 provides the composition and some relevant data for mortars. All the materials have been given a statistical characterization by means of a large number of tests [9,19,21–24] summarized in Table 2. The measured data reveal the great difference between cement (type 1 and 2) and lime (type 3) mortars as well as between modern and old bricks; the dispersion, lying somewhere in-between 15% and 30% of the average value, can be considered as typical for brickwork [25,26].

The brickwork specimens have been tested with load eccentricity of 0, 40, 60 (only for brickworks 1 and 2) and 80 mm and each test has been repeated at least twice. Fig. 2 shows the loading conditions together with the position of displacements transducers;

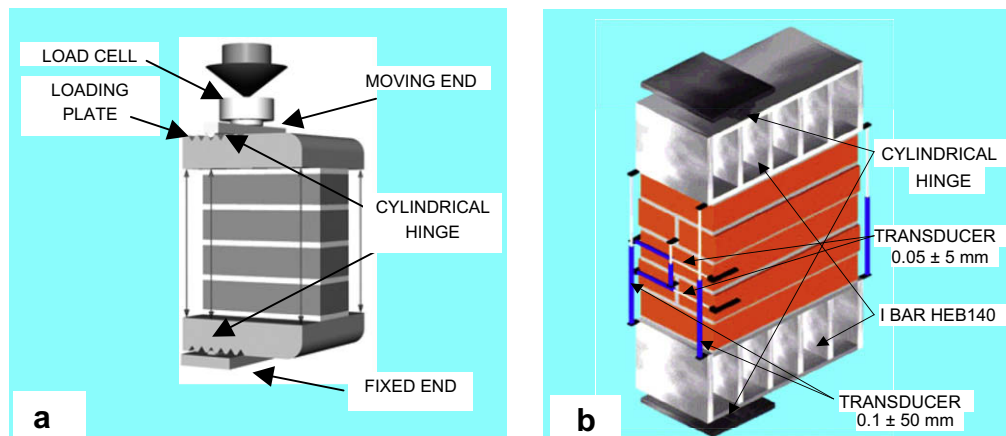


Fig. 1. Test set-up for: (a) specimen 1 and 2 and (b) specimen 3.

Table 2
Mechanical characteristics of bricks and mortars

Av. value (N/mm ²)	No. of samples	CoV (%)	Property	Av. value (N/mm ²)	No. of samples	CoV (%)
Mortar 1				Brick 1		
13.1	20	18	Compr. strength	19.7	20	17
1545	20	16	El. modulus (compr.)	1530	20	30
3.4	10	15	Tens. strength – TPB	4.7	10	10
1120	10	19	El. modulus (tensile)	920	10	25
0.98%	20	15	Strain at peak load	1.41%	20	21
Mortar 2				Brick 2		
10.0	20	16	Compr. strength	30.5	10	17
1365	20	22	El. modulus (compr.)	3920	10	25
2.7	10	12	Tens. strength – TPB	4.6	6	32
870	10	23	El. modulus (tensile)	1107	6	30
0.99%	20	18	Strain at peak load	0.94%	10	22
Mortar 3						
2.3	14	30	Compr. strength			
480	14	40	El. modulus (compr.)			
1.2	10	20	Tens. strength – TPB			
380	10	33	El. modulus (tensile)			
0.71%	14	22	Strain at peak load			

data taken from corresponding transducers on opposite sides of the specimen allowed a control of undesired lateral eccentricity.

2.2. External constraints of the specimen and eccentric loading

There are two ways for performing eccentric load tests on masonry prisms: a cylindrical hinge is located over the top plate and (i) another cylindrical hinge below the bottom one, Fig. 3a; (ii) the specimen directly built on a stiff base connected to the reaction frame, Fig. 3b. These two experimental set-up appear to be equivalent, but they are not.

In the first case, the forces transmitted by the plates to the specimen are easily calculated since the problem is statically determinate; this ensures that the force path is a straight line from one

hinge to the other making the specimen to be loaded with constant eccentricity throughout the height during the whole test.

In the second case, the loading on the specimen may have non-constant eccentricity as a consequence of testing details: it is sufficient that, thanks to friction, a shear force is allowed to develop for the problem to become redundant, since the distribution of the stresses at the base of the specimen and the position of load resultant are unknown; moreover, the eccentricity may vary during the test, without any possibility of measuring its position.

Fig. 4 shows the crack pattern of an eccentrically loaded specimen [4] at the end of a test performed according to the set-up of Fig. 3b. The diagonal crack shows that the load path was inclined from the top-left to the bottom-right corner of the specimen and therefore, in these conditions, the measured peak load is related to a non-constant load eccentricity.

In the present study, according to the purpose of obtaining an estimate of the load carrying capacity as a function of the load eccentricity, the tests have been performed according to Fig. 3a.

2.3. Experimental set-up

The testing set-up is presented in Fig. 1a for brickworks 1 and 2, in Fig. 1b for brickwork 3 being the three series of tests performed in different laboratories; minor details are omitted for simplicity [19,27]. All the tests have been performed with 10 Hz acquisition frequency, under displacement control with velocity $v_{min} = 0.01$ mm/s.

For brickworks 1 and 2 the load is measured with a 0.01% precision load cell while the relative displacements are measured by means of LVDT transducers with a 1/1200 mm precision; the displacement of the upper plate is measured directly below the load line, while the lateral ones are recorded close to the ends of the specimen in order to deduce the rotation of the plates. The lower hinge is fixed (connected to the testing frame) and the upper one (under the load cell) moved by means of a mechanical device. The load cell can be considered as a spring with high stiffness; up to the limit load this does not affect the results at all; it may alter the measurements only far after the material collapse, at a point when the softening curve has already lost any mechanical meaning. A 2 mm thick lead sheet between the specimen and the loading plates was used to smooth the bases of the specimens; friction between the bases and the loading plates could not be removed because eccentric loading without friction would result in highly unstable tests. The tests are displacement controlled being the displacement of the upper plate, below the load line, the controlled loading parameter.

A similar testing set-up (Fig. 1b) is used for brickwork 3, which comprises two steel bars ($\varphi = 30$ mm) as cylindrical hinges between the plates and the reaction frame, and two steel I bars HEB140, stiffened with vertical flanges, in contact with the bases of the specimen. In both the cases, the loading plates can be assumed rigid in comparison with the tested specimens. The load

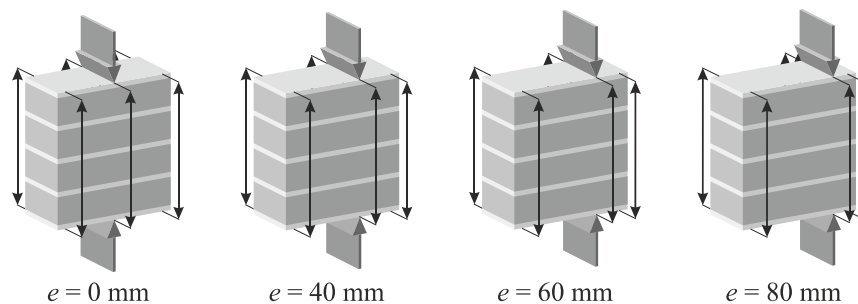


Fig. 2. Tested specimens: load eccentricities and displacement transducer positions.

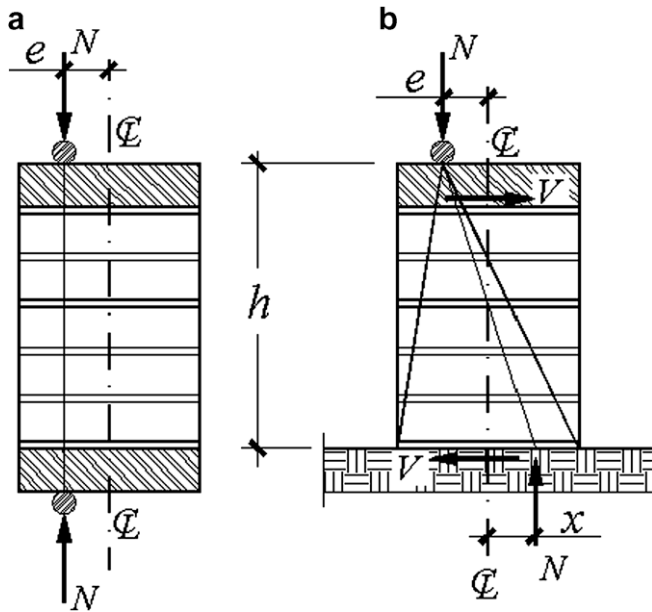


Fig. 3. Load-transfer schemes for eccentric loading tests: (a) double cylindrical hinge and (b) cylindrical hinge and fixed base.

is applied through the cylindrical hinges to the I bars, which are free to rotate. The I bars avoid a stress concentration on the specimen while providing the plane section condition at the bases of the masonry prism. The specimens have been instrumented with seven displacement transducers, four transducers (sensitivity 0.1 mm, operating range ± 50 mm) measured the relative displacement at the four edges of the steel bars, the other three being placed on the bricks, on the compressed side, to measure the local strain: two resistive transducers (sensitivity 0.05 mm, operating range ± 5 mm), were placed horizontally, one of which across the head mortar joint; the third one (sensitivity 0.07 mm, operating range ± 10 mm) in the vertical direction.

3. Test results

Fig. 5 shows the stress–strain response of the specimens for concentric loading, identified as $e = 0$, summarized in Table 3, while

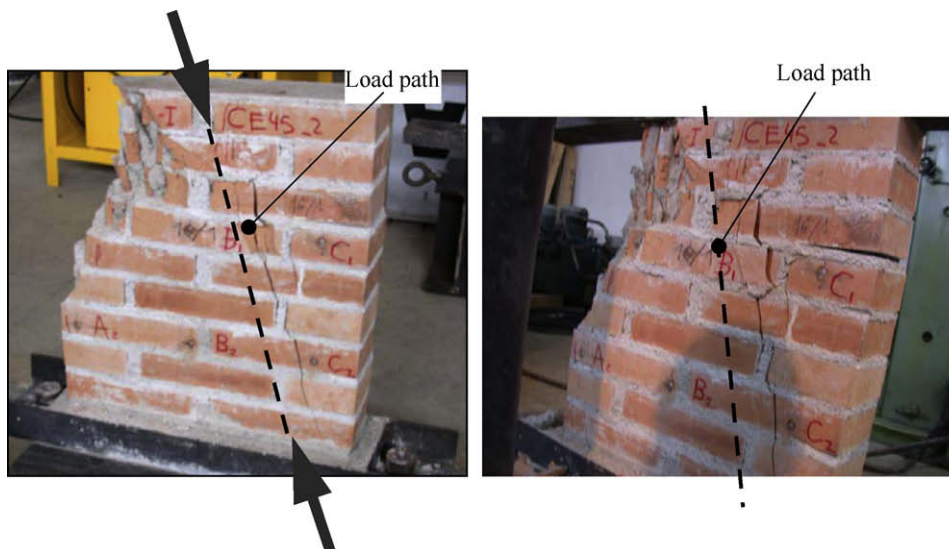


Fig. 4. Load paths in the specimen for cylindrical hinge and fixed base constraints (from Martinez, 2003, with permission from the author).

Figs. 6 and 7 refer to eccentric tests with eccentricity $e = 40$ mm, 60 mm (not for brickwork 3) and 80 mm, in terms of load–displacement and bending moment–curvature (i.e. relative rotation of the bases, divided by the height of the specimen) relationships.

The collapse mechanism of brickwork is showed in Fig. 8 (brickwork 1) and Fig. 9 (brickwork 3) for different values of the eccentricity. Collapse is characterized by crushing and successive spalling of external layers of the brick, with thickness of 10 mm on the average. This mechanism is due to a concentration of tensile stresses in the brick originating from the elastic mismatch between the brick and the joint. While for concentric tests the spalling is substantially uniform over the whole specimen, in the case of eccentric loading, the failure arises with crushing and spalling of the compressed edge of masonry; on the opposite side a crack develops at the brick/mortar horizontal interface (opening of the joint on the tensile side).

Specimens made with modern bricks (types 1 and 2 brickwork) exhibit a higher resistance, a clear linear elastic branch with a very limited pre-peak non-linear response and a sudden load decay in the post-peak branch. Specimens made with historical bricks (type 3) exhibit a lower resistance, a more pronounced non-linear pre-peak phase and a post-peak softening tail rather long where, despite the damage state, masonry reveals the capacity of sustaining loading–unloading cycles without appreciable stiffness degradation; this deformation capacity may play a significant role in safety assessment of eccentrically loaded structures, as will be shown in the next paragraphs.

4. Macroscopic constitutive models

The most common macroscopic models of masonry in compression are: (i) a no-tensile-resistant perfectly brittle model in compression (NTR-PB), Fig. 10a; (ii) a NTR elastic–perfectly plastic (NTR-PP) model with unbounded ductility, Fig. 10d. Both these models are characterized by two mechanical parameters only: the compressive strength f_c and the elastic modulus E . Both parameters may be defined by means of experimental tests or theoretical approaches; in the present case, for each type of brickwork, the compressive strength f_c and the elastic modulus E can be estimated from concentric load tests as the peak load-to-loaded area ratio ($f_c = N_c/A$) and the stress–strain ratio at 0.6 of the peak load, respectively. The simplicity of these models is somehow counterbalanced

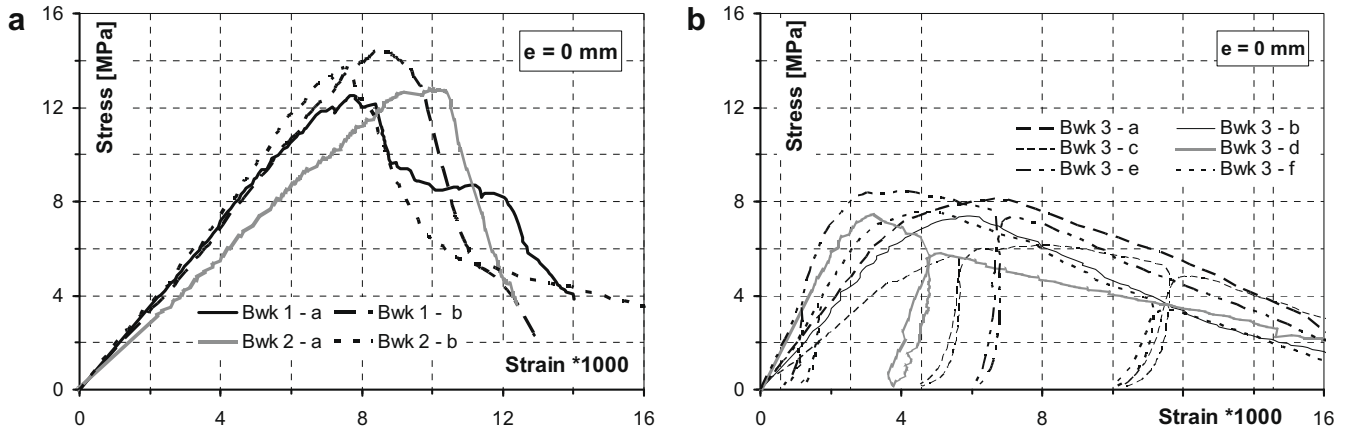


Fig. 5. Concentric loading for (a) brickwork 1 and 2 and (b) brickwork 3. Stress–strain diagrams.

Table 3
Concentric loading – summary of the experimental results

	f_c (MPa)	$\epsilon_c = \epsilon(f_c) \times 10^3$	E (MPa)
Brickwork 1			
Specimen – a	12.51	7.63	1866
Specimen – b	14.55	8.21	1867
Average	13.53	7.92	1867
Brickwork 2			
Specimen – a	12.78	10.23	1399
Specimen – b	13.66	7.27	2001
Average	13.22	8.75	1700
Brickwork 3			
Specimen – a	8.14	7.00	1882
Specimen – b	7.42	5.96	1776
Specimen – c	6.14	7.78	1303
Specimen – d	7.47	3.62	2843
Specimen – e	8.50	4.01	3430
Specimen – f	7.60	4.20	2643
Average	7.54	5.43	2313

by a reduced accuracy, since they do not properly take into account the inelastic compressive response of brickwork, that exhibits a first linear branch, Fig. 5, followed by an inelastic phase when approaching to the peak load and a subsequent descending branch where the load carrying capacity decreases with progressive cracking of the specimen.

In order to better represent the experimental behaviour, a constitutive model should therefore provide an adequate representation of the inelastic strains that develop in the pre- and post-peak phases. Fig. 10b and c shows two other macroscopic constitutive models for masonry: the elastic–plastic model with limited available ductility (NTR-EP) [9] and the Kent and Park model (K&P), [19,28]. Both models are simple enough for practical use in engineering applications being, at the same time, able of better representing the behaviour exhibited by brickwork.

The NTR-EP model, can be defined from concentric tests according to two simple rules: (i) the yielding point is given as the intersection of the elastic branch and yield plateau at the peak stress: $\epsilon_{el} = f_c/E$; (ii) the limit strain ϵ_l is such that the strain energy of the bilinear model, up to the limit strain, is equal to that of the experimental diagram, up to a load decay of 20%. The choice of the limit strain based on the proposed energy equivalence is somehow arbitrary and other more complex rules can be followed for

defining the bilinear model, however the differences are negligible for practical applications. The available ductility, defined as the ratio $\eta_{av} = \epsilon_l/\epsilon_{el}$ between the limit strain and the elastic strain, is a measure of the ductility capacity of the material and can be calculated from experimental tests with concentric loading. According to the experimental results presented in previous section, the available ductility lies in the range 1.2–1.3 for brickworks 1 and 2, and in the range 2.0–3.0 for brickwork 3 (see Table 4). The greater ductility of historical masonry displayed by the tests depends on both, historical brick fabric, and lime mortar characteristics, and is also confirmed by some other recent tests [29].

The Kent and Park (K&P) model consists of an ascending branch represented by a second-degree parabolic curve, a linear descending softening branch and a final constant branch [28]. Originally formulated for confined concrete, the model is defined by three parameters, namely the peak stress f_c , the corresponding strain $\epsilon_c = \epsilon(\sigma = f_c)$, the ultimate strain ϵ_u , i.e. the value reached at stress level $0.2 f_c$. Saying $\tilde{\sigma} = \sigma$ and $\tilde{\epsilon} = \epsilon/\epsilon_c$, the normalized stress and strain, respectively, the three branches of the model are given as

$$\begin{aligned} \tilde{\sigma} &= 2\tilde{\epsilon} - \tilde{\epsilon}^2, & \text{for } 0 \leq \tilde{\epsilon} \leq 1; \\ \tilde{\sigma} &= 1 - 0.8 \left(\frac{\tilde{\epsilon} - 1}{\eta - 1} \right), & \text{for } 1 \leq \tilde{\epsilon} \leq \eta; \\ \tilde{\sigma} &= 0.2, & \text{for } \tilde{\epsilon} \geq \eta \end{aligned} \quad (1)$$

where $\eta = \epsilon_u/\epsilon_c$. However, for the purposes of this work, the third constant branch is not considered in the analyses presented hereafter. The values of the K&P model parameters f_c , ϵ_c , ϵ_u , can be directly taken from experimental results as summarized in Table 4.

5. Compressive strength

The capability of the previously defined models to reproduce the experimental behaviour is addressed in this section by verifying that eccentric tests provide the same value of the material compressive strength as given by concentric experiments.

Concentric load tests can be assumed to produce a uniform stress distribution over the section, and therefore the compressive strength f_c can be defined as the peak load-to-loaded area ratio ($f_c = N_c/A$). Eccentric load tests, on the contrary, induce a stress distribution in the specimen that is unknown, leading to a statically indeterminate problem. As a consequence, the evaluation of the material compressive strength from eccentric tests needs two assumptions: (i) the strain distribution over the section, that can be assumed to be linear, as confirmed in previous experimental

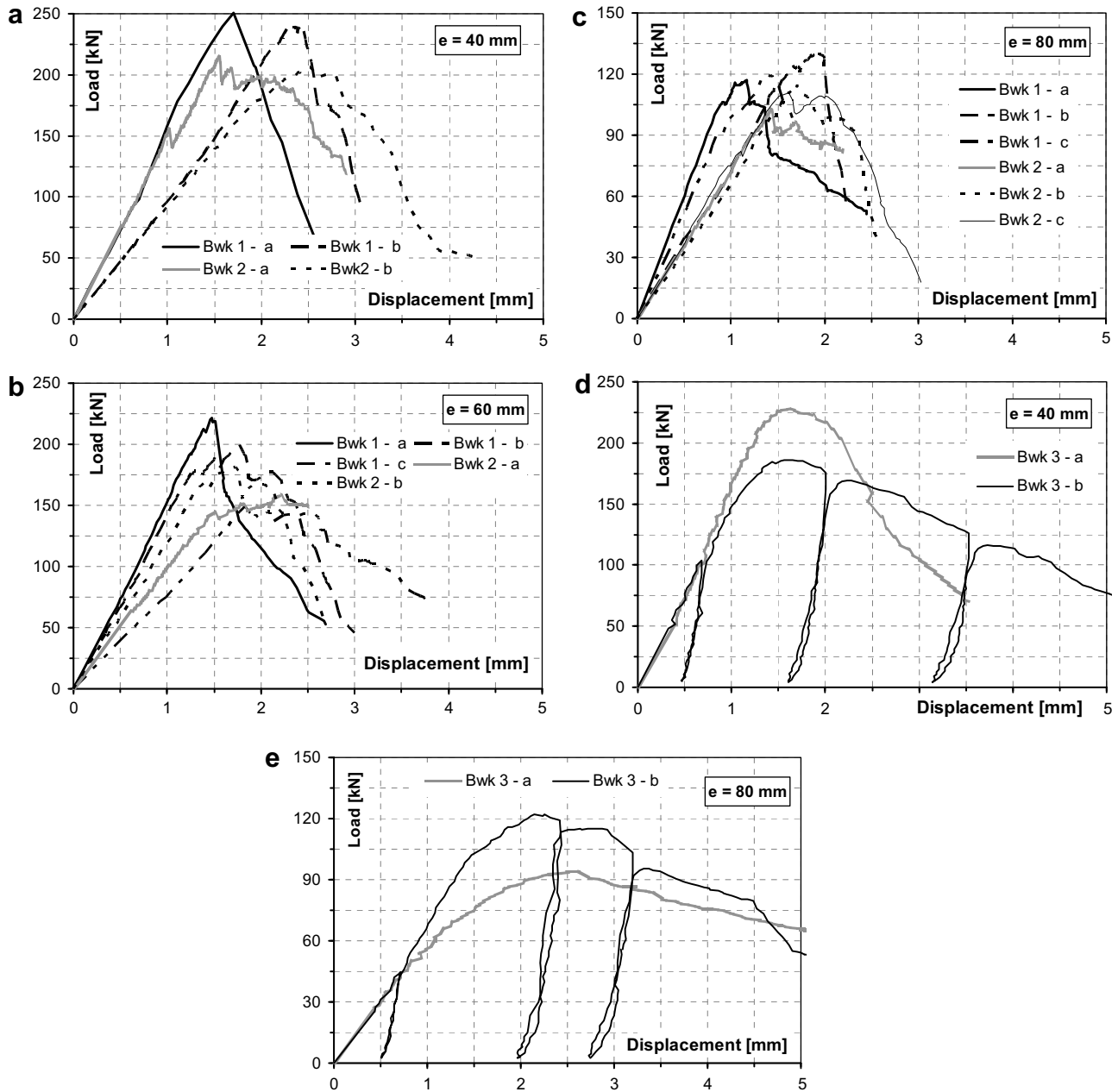


Fig. 6. Eccentric loading. Brickwork 1 and 2: (a) $e = 40$ mm; (b) $e = 60$ mm; (c) $e = 80$ mm. Brickwork 3: (d) $e = 40$ mm; (e) $e = 80$ mm. Load–displacement diagrams.

works (see for instance: [9]) and (ii) the constitutive model for the material, allowing a stress distribution to be deduced from the assumed strain distribution. It is therefore clear that the value of the compressive strength, if deduced from eccentric load tests, depends on the constitutive model assumed for masonry. In Table 5 the values of resulting compressive strength is deduced from eccentric tests is the case of the aforementioned constitutive models; despite the experimental strength variability, that is rather high when dealing with masonry specimens, the results clearly show that the compressive strength $f_c^{\text{NTR-PB}}$ deduced from a NTR-PB model increases with increasing of load eccentricity, while no strength increase results if the inelastic post-peak strains are considered, i.e. if the available ductility concept (NTR-EP) or the Kent and Park model are used to provide the compressive strength under eccentric loading. Therefore, the apparent increase showed by the elastic brittle model is a consequence of the simplified constitutive model adopted.

In detail, assuming a NTR-EP model with limited available ductility, Table 5 shows that brickwork 1 exhibits a compressive strength $f_c^{\text{NTR-EP}}$ of 12.9 N/mm^2 with a coefficient of variation (CoV) = 12%, brickwork 2 an average value of 12.0 N/mm^2 with CoV = 7%, and brickwork 3 a 7.8 MPa average strength with CoV = 25%. The low values of the coefficients of variation, but for brickwork 3, show the reliability of the proposed NTR-EP approach. It can be shown that the NTR-PB model, for partially compressed sections, overestimates the compressive strength $f_c^{\text{NTR-PB}}$ by a factor that depends on the available ductility (Fig. 11)

$$f_c^{\text{NTR-PB}} = \frac{2\eta_{av} - 1^2}{3\eta_{av}^2 - 3\eta_{av} + 1} f_c^{\text{NTR-EP}} \quad (2)$$

provided

$$\frac{e}{h} > \frac{1}{6} \frac{3\eta_{av} - 2}{\eta_{av}(2\eta_{av} - 1)} \quad (3)$$

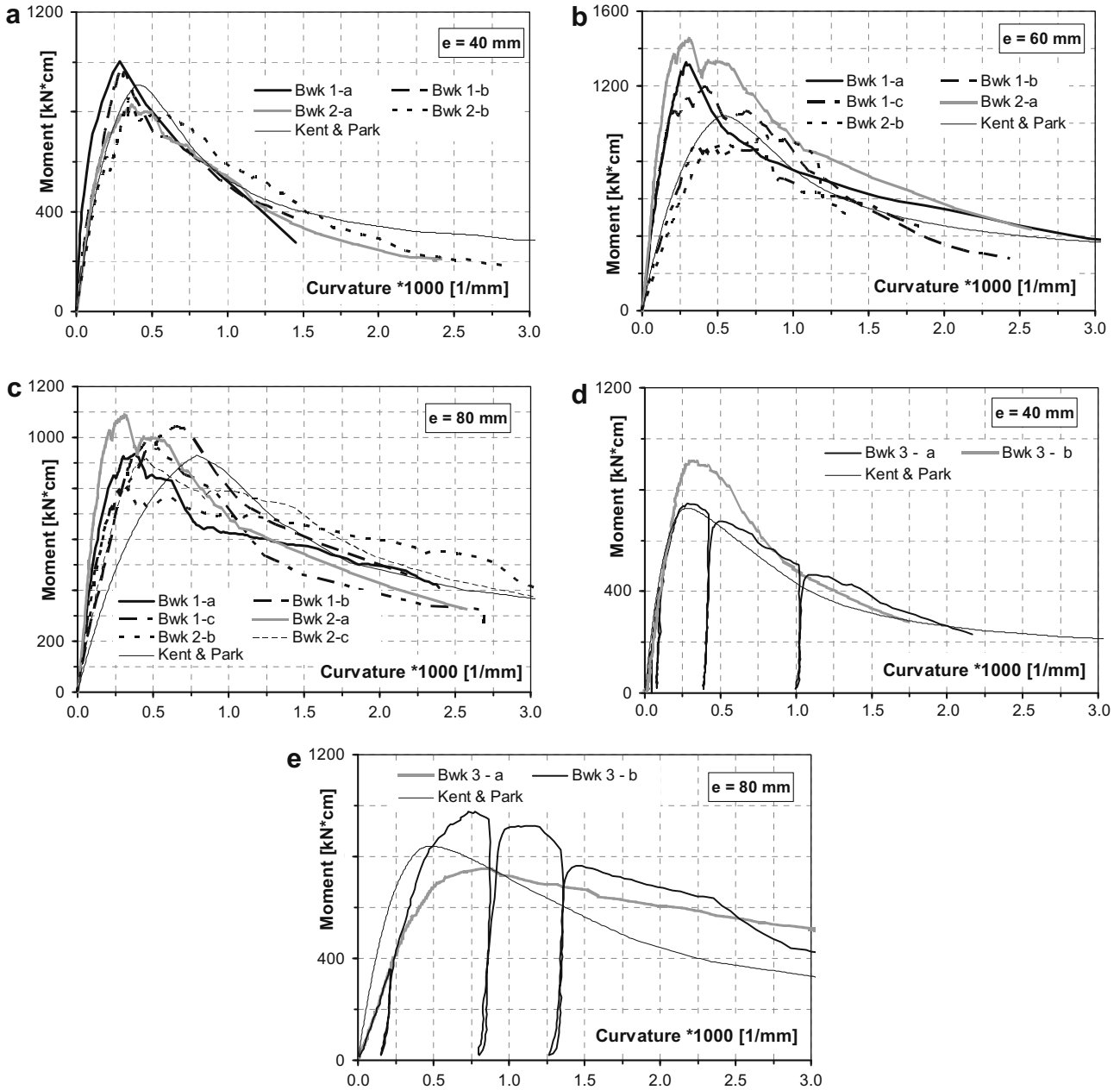


Fig. 7. Eccentric loading, Brickwork 1 and 2: (a) $e = 40$ mm; (b) $e = 60$ mm; (c) $e = 80$ mm. Brickwork 3: (d) $e = 40$ mm; (e) $e = 80$ mm. Bending moment–curvature diagrams.

which accounts for an apparent increase of the compressive strength up to 33% in the case of infinite ductility of an elastic–perfectly plastic material.

6. Force–displacement and moment–curvature diagrams

The performances of both, the NTR-EP, Fig. 10b, and the K&P, Fig. 10c models in terms of stress–strain and moment–curvature behaviour are compared to experiments in Fig. 12.

In the case of concentric loading (Fig. 12a and b) it has to be noted that for specimens made with modern brickwork (types 1 and 2) the peak load is reached almost directly after a linear elastic branch, while for the specimens made with old bricks (type 3) a marked non-linear behaviour appears when approaching to the peak load. Therefore, the K&P model, while reproducing accurately the experimental behaviour of brickwork 3 (Fig. 12b) in both

ascending and descending branches, fails in fitting the experimental curve of brickwork 1 and 2 (Fig. 12a). On the contrary the NTR-EP model fits well the response close to the peak load, especially for brickworks 1 and 2, thanks to the sharp transition between the linear elastic branch and plastic plateau, while giving only a coarse description of the post-peak behaviour.

Relying on the Navier–Bernoulli assumption of plane section under axial force and bending moment, the previously defined uniaxial stress–strain models, whose mechanical parameters have been calibrated according to concentric tests, can be integrated over the section in order to provide the behaviour of masonry under eccentric loading. As shown in Fig. 12c and d, significant differences between the models arise in this case:

- the NTR-PB model (Fig. 10a) is unable in representing neither the peak load nor the post-peak softening branch;

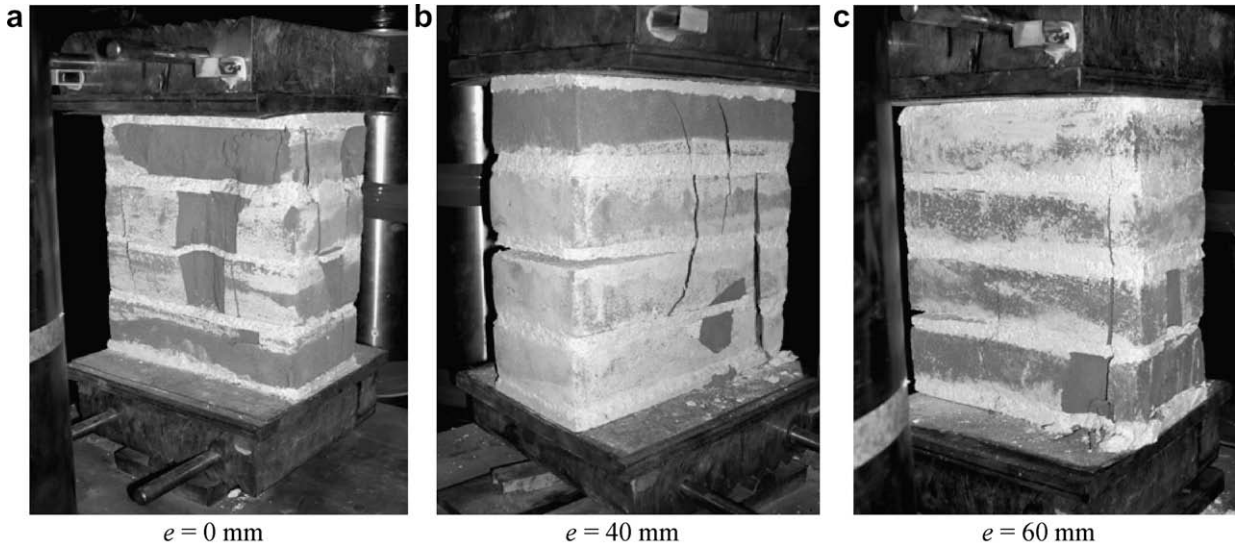


Fig. 8. Collapse mechanism for brickwork 1 under concentric and eccentric loading.

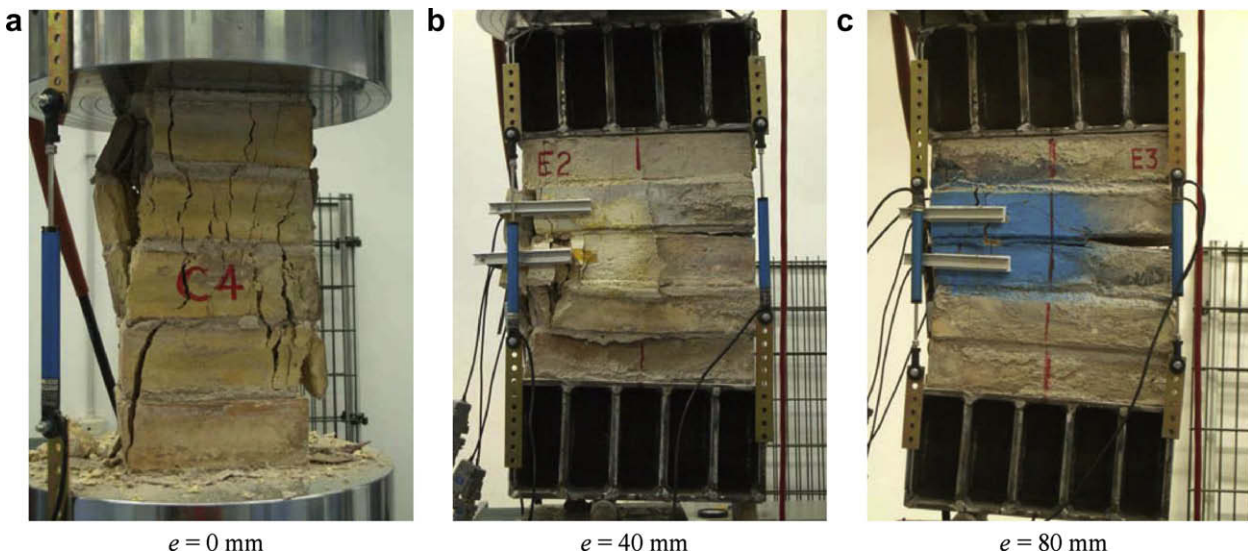


Fig. 9. Collapse mechanism for brickwork 3 under concentric and eccentric loading.

- the NTR-EP approach (Fig. 10b) provides a good estimate of the pre-peak branch; a good agreement with the test data is found also in the post-peak branch in the case of high load eccentricity, while a higher discrepancy is recognized for lower eccentricities and
- the K&P model (Fig. 10c) is able to fit the experimental data with good agreement in both the pre-peak and post-peak branches.

7. Limit domains

For assessment purposes, the experimental results under eccentric loading can be better represented in a $N/N_0 - M/M_0$ plane, where, for each brickwork type, the normalising quantities N_0 and M_0 are, respectively, the average ultimate load obtained under concentric loading $N_0 = \langle N_c \rangle = \langle f_c \rangle A$, and the ultimate bending moment $M_0 = N_0 b/4$. The limit domain for the NTR-PP model of Fig. 10d (steel-like material) is the solid bold parabola of Fig. 13, while the limit domain for the NTR-PB model (brittle material) is

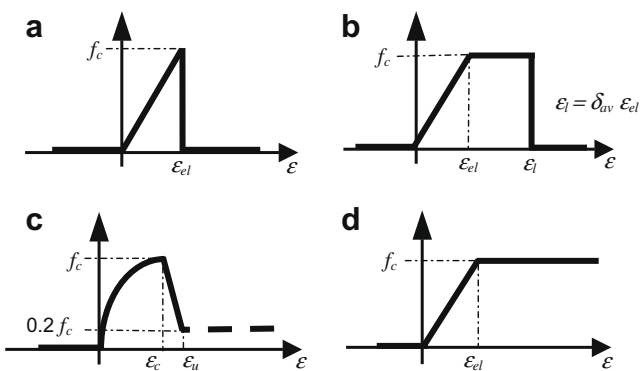


Fig. 10. No-tensile-resistant stress-strain relationships for masonry. (a) Perfectly brittle (NTR-PB); (b) elasto-plastic with limited ductility (NTR-EP); (c) Kent & Park (K&P); (d) elastic-perfectly plastic with unlimited ductility (NTR-PP) models.

Table 4
Concentric loading – parameters for the constitutive models

	Elastic–plastic lim. duct.			Kent & Park		
	$\epsilon_{el} \times 10^3$	$\epsilon_l \times 10^3$	$\eta_{av} = \epsilon_l/\epsilon_{el}$	f_c (MPa)	$\epsilon_c \times 10^3$	$\epsilon_u \times 10^3$
Brickwork 1						
Specimen – a	6.70	8.50	1.27	12.51	7.63	14.9
Specimen – b	7.79	9.53	1.22	14.55	8.21	12.6
Average	7.25	9.01	1.25	13.53	7.92	13.7
Brickwork 2						
Specimen – a	9.14	10.83	1.19	12.78	10.23	12.5
Specimen – b	6.83	8.20	1.20	13.66	7.27	12.0
Average	7.98	9.51	1.19	13.22	8.75	12.2
Brickwork 3						
Specimen – a	4.32	9.73	2.25	8.14	7.00	17.1
Specimen – b	4.18	8.33	1.99	7.42	5.96	15.0
Specimen – c	4.71	11.72	2.49	6.14	7.78	21.4
Specimen – d	2.63	5.03	1.91	7.47	3.62	17.0
Specimen – e	2.48	8.07	3.26	8.50	4.01	16.8
Specimen – f	2.88	7.35	2.56	7.60	4.20	15.4
Average	3.53	8.37	2.41	7.54	5.43	17.1

represented by the inner bold solid grey curve; dots represent the experimental data of the present experimental research.

The other curves in Fig. 13 are obtained with the NTR-EP model, for different values of the available ductility ($\eta_{av} = 1.15$, $\eta_{av} = 1.4$, $\eta_{av} = 2$), showing that an even moderate ductility induce a relevant widening of the limit domain, if compared to the perfectly brittle limit curve. The limit domains best fitting the experimental data are the ones taking into account a moderate available ductility between 1.15 and 1.4 for brickworks 1 and 2, and around 2.0 for brickwork 3. These outcomes are not unexpected since masonry and its constituents are known to be quasi-brittle, but not perfectly brittle materials.

Table 5
Ultimate load and compressive strength of all the specimens

Eccentricity (mm)	0		40		60			80		
Eccentricity/brick height	$e/h = 0$		$e/h = 1/6$		$e/h = 1/4$			$e/h = 1/3$		
Specimen	a	b	a	b	a	b	c	a	b	c
Brickwork 1										
N_u^{EXP} (kN)	375	436	251	242	221	199	150	117	131	119
f_c^{NTR-PB} (MPa)			16.4	15.8	18.9	17.0	12.8	14.4	16.2	14.7
f_c^{NTR-EP} (MPa) ($\delta_{av} = 1.2$)	12.5	14.5						12.0	13.4	12.2
$f_c^{K\&P}$ (MPa)			13.6	13.61	15.7	14.1	10.6	12.1	13.5	12.3
Brickwork 2										
N_u^{EXP} (kN)	384	410	214	206	158	181	102	115	111	
f_c^{NTR-PB} (MPa)			14.9	13.4	13.5	15.5	12.6	14.2	13.7	
f_c^{NTR-EP} (MPa) ($\delta_{av} = 1.2$)	12.8	13.7	11.6	11.1	11.2	12.8	10.4	11.7	11.3	
$f_c^{K\&P}$ (MPa)			11.6	11.2	11.3	12.9	10.6	11.8	11.4	
Brickwork 3										
N_u^{EXP} (kN)	149	134	103	108	164	138	186	229	95	122
f_c^{NTR-PB} (MPa)					9.4	12.0	9.4	12.0	8.6	11.3
f_c^{NTR-EP} (MPa) ($\delta_{av} = 2.0$)	8.1	7.4	6.1	7.5	8.5	7.6	7.5	9.2	6.9	9.0
$f_c^{K\&P}$ (MPa)					7.9	9.6	7.9	9.6	6.3	8.3
Note	Tests on half-brick specimens						Tests on full-brick specimens			

The solid black line with dots represents the K&P limit domain according to the constitutive parameters recalled in Table 4. The domain is close to the NTR-EP one with limited ductility $\eta_{av} = 1.4$ and is almost insensible to the limit strain ϵ_u within the experimental range of the performed tests ($12 \times 10^{-3} \leq \epsilon_u \leq 21 \times 10^{-3}$); therefore, it can be considered a somehow average domain in-between the brittle and ductile domains, as derived for the NTR-PB and NTR-PP models, that takes into account the inelastic phenomena on the average. Such behaviour can be explained referring to Fig. 14, that shows the K&P limit domains for different slope of the descending branch. Only a slight effect in terms of limit domain arise from the slope of descending branch, since the main contribution derives from the non-linear strains taken into account by model with the parabolic curve of the ascending branch; it is shown that an even brittle model (model K&P – 1), with a sudden decay after the peak load, leads to a limit domain that is much wider than the elastic–perfectly brittle (NTR-PB) one.

Fig. 15 is similar to Fig. 13, with the addition of the experimental data available from literature [2,3,8,9] showing that also solid concrete brickwork [2,3] and solid tuff stone brickwork [10] in the normalized $N/N_0-M/M_0$ plane, exhibit a behaviour similar to solid clay brickwork.

It seems surprising that some of the experimental points lie outside the limit domains, also considering that the domain for perfectly plastic materials should represent an upper bound of the effective strength. This outcome is due to a couple of reasons: (i) the effective eccentricity of the specimen is different from what expected, due to some bias in the experimental set-up and (ii) the compressive strength of the specimen is different from the average value that has been used for the normalising quantities N_0 and M_0 employed in the limit domains.

On the latter issue, it should be noted that the limit domains refer to the average value $\langle f \rangle$ of the material strength, which is a random variable. Taking into account a $\pm 10\%$ variation of compressive strength, the outer and inner dashed parabolas of Fig. 13 are

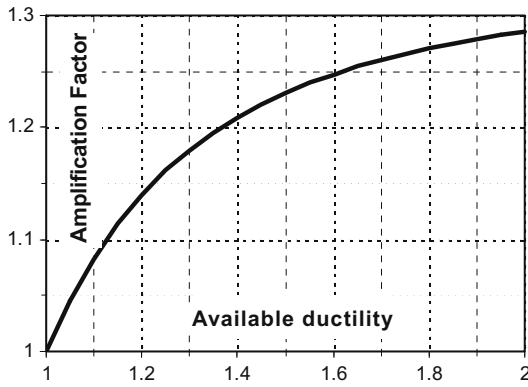


Fig. 11. Compressive strength amplification factor as a function of material available ductility, Eq. (2).

obtained for both the perfectly brittle, Fig. 10a, and perfectly plastic, Fig. 10d, materials: almost all the experimental points lie within these limits, the few external points are related to specimens that exhibited exceptionally high or low strength, as sometimes may happen in masonry related tests, showing the effect of uncertainty in building the limit domains.

The UIC code [7] asks NTR-PB models to be used for the assessment of railway masonry bridges, allowing an increase of brickwork compressive strength as the load eccentricity e/b is increased as shown in Fig. 16. The increase is allowed for medium to high eccentricity and might be as large as 60%, which makes the $N/N_0-M/M_0$ limit domain to be enlarged as represented in Fig. 15. Such a widened domain includes an area, for high eccentricities,

inside which several experimental points are found: this means that the enlarged domain assumes as safe a region where, on the contrary, several collapses have been recorded. Since the collapse of an arch, or an arch barrel in the case of a bridge, takes place when the axial thrust is highly eccentric in some sections (what is usually called a plastic hinge), the widened UIC domain appears to overestimate the load carrying capacity of arches and, therefore, to be unsafe. It is worthwhile noting that Euro Code 6 [30] does not allow any strength increase at all.

8. Discussion and conclusions

The experimental results presented in this paper provide an overall view of the compressive strength and the failure mechanisms of solid clay brickwork for varying eccentricity of the applied load. The comparison between the different types of brickwork shows that that masonry made with old bricks and lime mortar (brickwork 3) display a higher ductility with a non-linear branch before the peak load and a subsequent long softening branch; conversely, masonry with contemporary bricks (brickwork 1 and 2) display a linear behaviour up to the attainment of the limit load, a small plastic plateau and then a rapidly descending softening branch. The tests on both the kinds of brickwork, however, show that masonry in compression does not behaves as a perfectly brittle material: the even small ductility exhibited in the experiments turns out to be prominent in the case of non-uniform compression (eccentric loading).

The experimental behaviour have been reproduced taking into account the inelastic strains in masonry close and after the peak load; to this end, simple macroscopic constitutive models suitable for engineering applications, based on an uniaxial non-linear

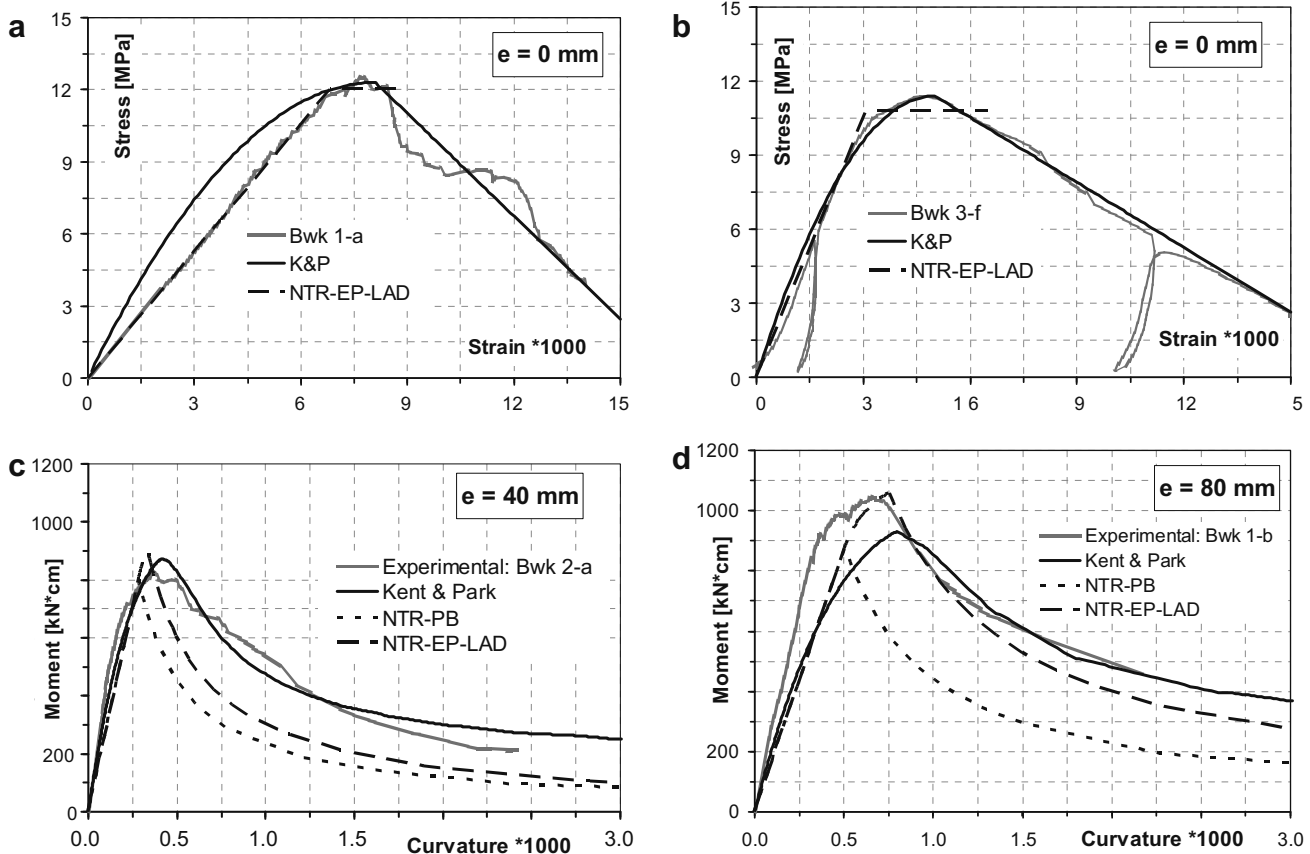


Fig. 12. Experimental and theoretical (NTR-EP + K&P models) response for concentric tests: (a) brickwork 1-a and (b) brickwork 3-f, and for eccentric tests: (c) $e = 40$ mm brickwork 2-a; (d) $e = 80$ mm brickwork 1-b.

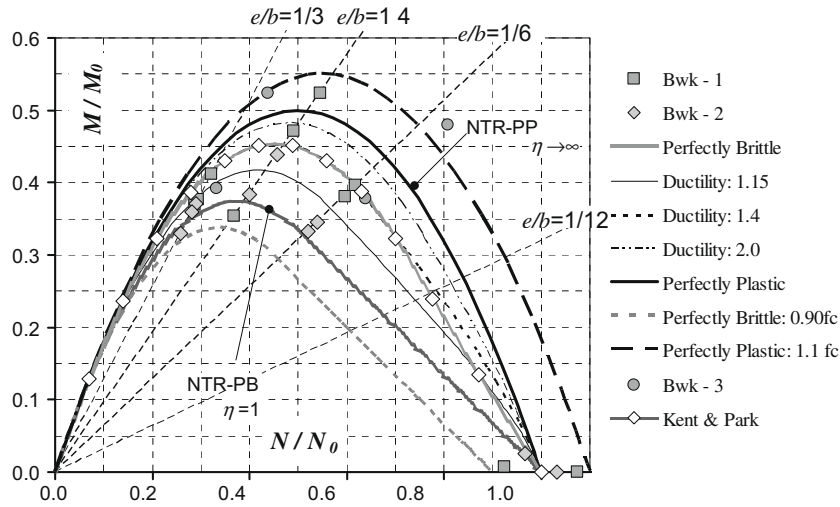


Fig. 13. Limit domains of the NTR-models: experimental data and homogeneous NTR-EP models with different available ductility.

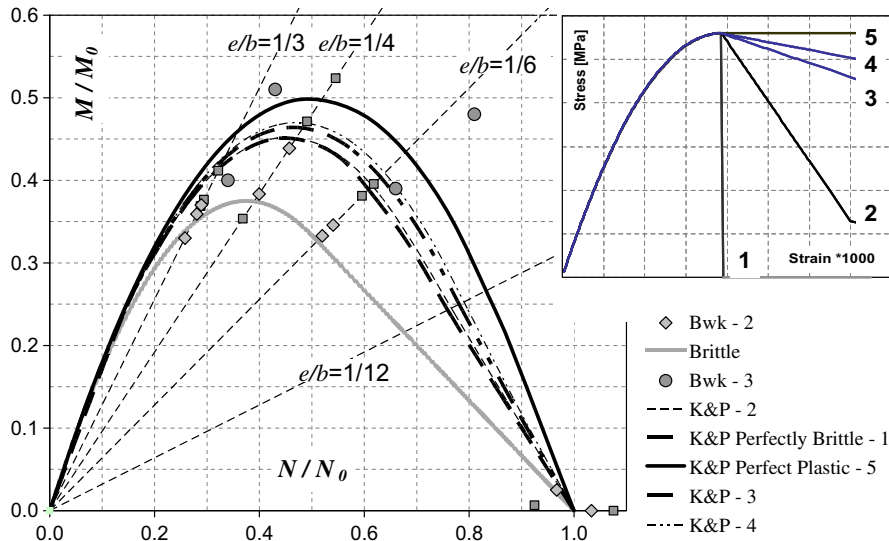


Fig. 14. Limit domains of K&P models for varying slope of descending branch from brittle (model 1) to perfect plastic (model 5) behaviour: comparison with experimental data.

stress-strain relationships in compression, together with the Navier-Bernoulli assumption of plane section, are shown to reproduce the experimental outcomes with reasonable precision and low computational requirements.

The limit domain in the axial force-bending moment plane can be estimated with rather good approximation, well below the experimental error, by means of an elastic-plastic model with limited ductility (1.2 for contemporary brick masonry and 2.0 for old clay brick masonry). The greater detail provided by the K&P model, which takes into account a non-linear pre-peak phase and an inelastic softening branch, while being useful in step-by-step prediction analyses, does not provide a significant improvement in terms of limit domain, with respect to the previously mentioned NTR-EP model. Whatever the constitutive model assumed for brickwork, the load bearing capacity under eccentric loading could be estimated from concentric tests, provided that inelastic strains that develop are properly taken into account. The increase of the

material strength for eccentric loading is shown to be only apparent and no amplification factor is therefore required.

The limit domains are significantly influenced by the material compressive strength, so that a small increase or decrease, as large as 10%, may lead to significantly widened or reduced limit domains. As a consequence, the material strength variability should be careful taken into account in order to define safe domains for assessment purposes.

Therefore, aiming at estimating the load carrying capacity of masonry structures under eccentric loading, on the one side, the appropriate material ductility should be considered in order to correctly reproduce the behaviour under eccentric loading but, on the other side, a convenient reduction factor should be applied to the material strength in order to get a conservative estimate of load bearing capacity. These conclusions may be of great importance for the assessment of arches and masonry arch bridges, especially for shallow or long spanning bridges, where crushing of masonry

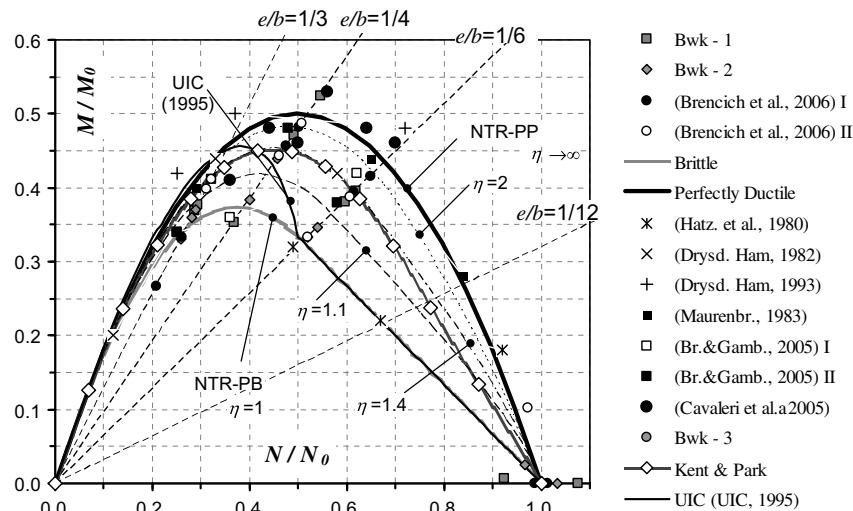


Fig. 15. Limit domains of the NTR-models with limited ductility: comparison with experimental data and the UIC (1995) domain.

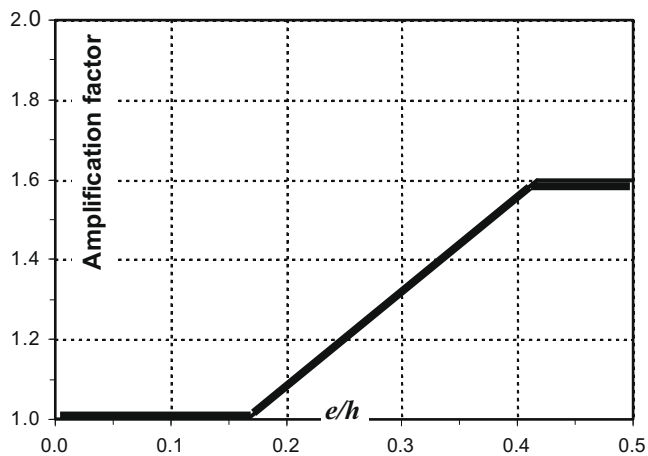


Fig. 16. Amplification factor of the compressive strength as a function of load eccentricity (from UIC code 778-3R, 1995).

under eccentric loading may be expected to activate the structural collapse.

Acknowledgments

The authors acknowledge the financial contribution by Italian Network of Seismic Laboratories (RELUIS) – 2005–2008 Pr., L3: “Safety assessment and vulnerability reduction of existing bridges” and L1: “Safety assessment and vulnerability reduction of masonry buildings”.

References

- [1] Hatzinikolas M, Longworth J, Warwaruk J. Failure modes for eccentrically loaded concrete block masonry walls. *ACI J* 1980;77:258–63.
- [2] Drysdale RG, Hamid AA. Effect of eccentricity on the compressive strength of brickwork. *Proc Brit Ceram Soc* 1982;30:140–8.
- [3] Drysdale RG, Hamid AA. Capacity of concrete block masonry prisms under eccentric compressive loading. *ACI J* 1983;80:102–8.
- [4] Martinez JLM. Theoretical and experimental determination of the limit domains of masonry structures, and application to historical structures. PhD thesis, T. U. of Madrid, Madrid, Spain, 2003 [in Spanish].
- [5] Martin Caro JA. Masonry compressive strength enhancement under eccentric axial load. In: Proceedings of the 4th arch bridge conference, Barcellona, 2004. Barcellona: CIMNE; 2004. p. 405–12.
- [6] Roberts TM, Hughes TG, Dandamudi VR, Bell B. Quasi-static and high cycle fatigue strength of brick masonry. *Constr Build Mater* 2006;20:603–14.
- [7] UIC – International Union of Railways: UIC code 778-3R. Recommendations for the assessment of the load carrying capacity of the existing masonry and mass-concrete arch bridges, 1995.
- [8] Maurenbrecher AHP. Compressive strength of eccentrically loaded masonry prisms. In: Proceedings of the 3rd Can Mas Symposium, Edmonton, 10/1–10/13, 1983.
- [9] Brencich A, Gambarotta L. Mechanical response of solid clay brickwork under eccentric loading. Part I: unreinforced masonry. *Mater Struct RILEM* 2005;38:257–66.
- [10] Cavaleri L, Failla A, La Mendola L, Papia M. Experimental and analytical response of masonry elements under eccentric vertical loads. *Eng Struct* 2005;27:1175–84.
- [11] Hilsdorf HK. Investigation into the failure mechanism of brick masonry under axial compression. In: Johnson FB, editor. *Proc Des Eng Constr Mas Prod*. Houston (TX): Gulf Publishing; 1969.
- [12] Francis AJ, Horman CB, Jerrems LE. The effect of joint thickness and other factors on the compressive strength of brickwork. In: *Proc 2nd IBMaC*, Stoke on Kent, 1971.
- [13] Khoo CL, Hendry AW. A failure criteria for brickwork in axial compression. In: *Proc 3rd IBMaC*, Essen, 1973. p. 141–5.
- [14] Atkinson RH, Noland JL. A proposed failure theory for brick masonry in compression. In: *Proc of the 3rd Can Mas Symp*, Edmonton, 1983.
- [15] Rots JG. Numerical simulation of cracking in structural masonry. *Heron* 1991;36:49–63.
- [16] Biolzi L. Evaluation of compressive strength of masonry walls by limit analysis. *J Struct Eng, ASCE* 1988;114:2179–89.
- [17] Milani G, Lourenço PB, Tralli A. Homogenised limit analysis of masonry walls. Part I: failure surfaces. Part II: structural examples. *Comput Struct* 2006;84:166–95.
- [18] Castigliano CAP. *Theorie de l'equilibre des systeme elastique et ses application*. Torino: Negro Ed.; 1879.
- [19] de Felice G. Experimental behaviour of brick masonry under axial load and bending. In: *Proc 7th Int Mas Conf*, London, 2006.
- [20] Boothby TE. Load rate of masonry arch bridges. *J Bridge Eng, ASCE* 2001;6:79–86.
- [21] prEN 772-1.2002. Methods of test for masonry units – part 1: determination of compressive strength, October 2002.
- [22] prEN 998-2.2004. Specification for mortar for masonry. *Masonry mortar*, March 2004.
- [23] prEN 1015-11.2001. Methods of test for mortar for masonry – part 11: determination of flexural and compressive strength of hardened mortar, June 2001.
- [24] prEN 1052-1.2001. Methods of test for masonry – part 1: determination of compressive strength, January 2001.
- [25] Ellingwood B, Tallin A. Limit states criteria for masonry construction. *J Struct Eng, ASCE* 1985;111:108–22.
- [26] Dymiotis C, Gutteder BM. Allowing for uncertainties in the modelling of masonry compressive strength. *J Constr Build Mater* 2002;16:443–52.
- [27] Corradi C. Theoretical and experimental analysis of the strength of eccentrically loaded brickwork. PhD thesis, Department Str and Geotech Eng, University of Genoa, Italy, 2006 [in Italian].
- [28] Kent DC, Park R. Flexural members with confined concrete. *J Struct Div, ASCE* 1971;97(7):1969–90.
- [29] Brencich A, Morbiducci R. Masonry arches: historical rules and modern mechanics. *Int J Archit Heritage* 2007;1(2):165–89.
- [30] ENV 1996-1-1. EURO CODE 6. Design of masonry structures, part 1-1: general rules for buildings – rules for reinforced and un-reinforced masonry, 1996.